STRUCTURE LASER BEAM IN NON-HOMOGENEOUS ENVIRONMENT

Krystof POLAK, CERN, Geneva, Switzerland and TUL, Liberec, Czech Republic
Jean-Christophe GAYDE, CERN, Geneva, Switzerland
Miroslav SULC, TUL, Liberec, Czech Republic and IPP, Praha, Czech Republic

Abstract

This article summarizes part of the research related to the structured laser beam (SLB) properties focused on alignment. The SLB has the potential to be used as a reference line. This is due to SLB features such as a very clear spot in the center of the beam, a sharp boundary of the central spot, low divergence of the central spot (practically measured value 10 μrad) and theoretically infinite range (tested over several hundred meters). However, the environment (the non-homogeneous distribution of the refractive index) affects the trajectory of the SLB, which is then a general curve. A new approach based on numerical simulations was used to investigate this phenomenon. A method generalizing the diffraction integral was developed to trace accurately any optical beam in a non-homogeneous environment. This solution offers in principle a better accuracy than the Eikonal equation used for ray tracing because it allows evaluating the position of the optical beam center with methods based on the analysis of the optical intensity transverse distribution. The propagation of the complex amplitude in the longitudinal direction can generally not be described by the Eikonal equation, but the generalized diffraction integral attains this goal. The article compares the trajectories of a SLB calculated using both the Eikonal equation and the generalized diffraction integral. It describes the differences between these two approaches and identifies conditions under which these differences are negligible in an inhomogeneous environment. Furthermore, the influences of different types of environmental non homogeneities on the SLB trajectory are discussed.

INTRODUCTION

For the purpose of alignment, special forms of optical beams, so-called non-diffracting optical beams such as the Bessel beam (BB), have recently been used [1][2][3]. However, the use of BB has the disadvantage of a limited range. Under standard conditions, the longitudinal range does not exceed 20 m. This practically makes the BB unusable for long-range metrology.

However, a new type of optical beam was discovered, the so called Structured Laser Beam (SLB) [4]. The advantages of this beam lie in its cheap and simple generation and theoretically unlimited longitudinal range, which was practically tested over several hundred metres. Thus, it seems to be a suitable candidate for a high precision long range alignment system, for example, in the domain of particle accelerators. It is expected that under ideal conditions in a vacuum, SLB will propagate in a perfectly straight line

This article is about the influence on the SLB straightness of non-ideal conditions of propagation. Non-ideal conditions in this case mean a non-homogeneous distribution of the refractive index, which in this case is given by a non-homogeneous temperature distribution. The results presented in this paper are based on numerical simulations of optical beam propagation. For this purpose, it was necessary to create a new method that allows this type of simulations. Existing methods such as the Eikonal equation or Ray tracing used in plasma physics only trace rays and do not allow the calculation of the distribution of the beam's optical intensity in the transverse plane at a given distance. The new method, later referred to as the Generalized Diffraction Integral (GDI), allows the calculation of the optical intensity in the transverse plane and therefore allows the application of beam center detection algorithm. In principle, differences in beam center detection are expected when using either ray tracing methods or GDI.

Three different models of propagation medium were considered during the simulations. In the first model, only a linear temperature change in the vertical axis y was considered, and the gradient was zero in the other axes. The general temperature distribution in the second and third models is based on data from measurements made in the Transfer Tunnel 1 (TT1) and in the LHC tunnel at CERN. Both models assume a zero gradient in the horizontal axis x.
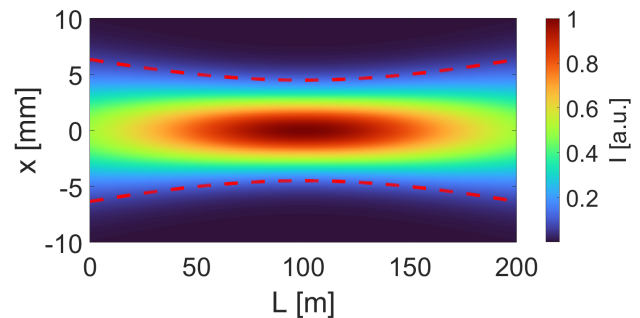

Figure 1: Longitudinal profile of the optimal GB. Dashed red curves indicate the radius of GB.

For simulations presented in this work only two different types of optical beams have been considered on a 200 m long alignment window. One of the optical beam is a Gaussian beam (GB) with a wavelength of $\lambda = 632.8$ nm optimized on the alignment window. The process of finding the optimal GB is described in [5] and the longitudinal profile of this GB is shown in the Figure 1. The second type of optical beam which is used is a SLB and is generated by an optical arrangement with an exit lens aperture of the same size as the exit lens aperture of the collimator for the optimal GB as referred in [5]. Longitudinal profile of the SLB field amplitude is visualised in the Figure 2.
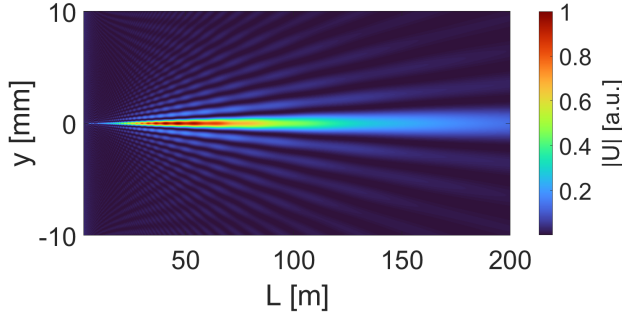
Figure 2: Longitudinal profile of the SLB field amplitude obtained from numerical simulations.

THEORETICAL BACKGROUND, NEW APPROACH AND METHODOLOGY

In this chapter, known theory for tracing of the light, namely Eikonal equation and Diffraction integral, are shortly explained, as well as the new proposed one based on the generalization of the Diffraction integral aiming at light tracing. Methodology for beam position detection and for calculation of refractive index of the environment are also discussed.
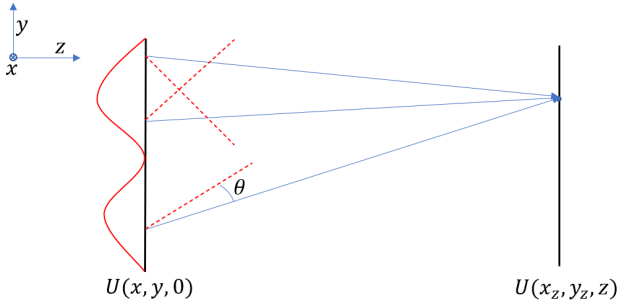
Diffraction integral

Figure 3: Illustration of the diffraction integral principle.

The diffraction integral can be derived from the wave equation via the transfer function [6]. However, another approach to its derivation based on Huygens' principle is presented below. This approach is more suitable for the subsequent generalization of the diffraction integral. The principle of the diffraction integral is illustrated in the Figure 3. According to Huygens' principle, each point of the wavefront can be considered as a source of spherical waves. This consideration generally means that every point of the optical field in the transverse plane is a source of spherical wave with the phase of the optical field. So, the point $[x_z, y_z]$ in the transverse plane at distance z is calculated as the sum of all contributions from the known field in the transverse plane at the origin. The solid red curve represents the phase of the optical field in the transverse plane at the origin, and the dashed red lines represent the perpendicular to the phase at that point. This principle can be written using

a relation

$$U(x_z, y_z, z) = \iint_{-\infty}^{\infty} U(x, y, 0) \frac{\exp(ikr)}{r} K(\theta) dx dy,$$
(1)

where U is a complex amplitude of the scalar optical field, r is a length of the radius vector of the specific spherical wave from point $[x, y, 0]$ to $[x_z, y_z, z]$ and $K(\theta)$ is the so-called inclination factor. The inclination factor has a phase and an amplitude. The phase depends on the cosine of the angle θ, i.e. the angle between the radius vector $\vec{r}$ and the normal vector to the phase, see Figure 3. The amplitude of the inclination factor is i/λ, so

$$K(\theta) = \frac{i}{\lambda} \cos(\theta).$$
(2)

After substituting the inclination factor into the equation (1), the diffraction integral has the form

$$U(x_z, y_z, z) = \frac{i}{\lambda} \iint_{-\infty}^{\infty} U(x, y, 0) \frac{\exp(ikr)}{r} \cos(\theta) dx dy.$$
(3)

Eikonal equation and Ray Tracing

The description of light tracing through a non-homogeneous medium is more complex. It is practically impossible to solve the wave equation directly over large distances. Thus, current methods move from a wave concept of optics to a geometric concept of optics, which considers light as rays.

One of the known methods introduces at the level of wave optics the so called Eikonal $S(x, y, z)$, for which a given point in space represents the path of a given solution of the wave equation in a non-homogeneous environment. Places with a constant value of S represent wavefronts. Then, the Eikonal equation [6][7] can be deduced

$$(\nabla S)^2 = n^2.$$
(4)

If the path of the ray $s(x, y, z)$ is introduced, whose trajectory is perpendicular to the wavefront at all points, the equation (4) can be rewritten into the ray equation

$$\frac{d}{ds} \left(n \frac{d\vec{r}}{ds} \right) = \nabla n.$$
(5)

For the solution in the longitudinal direction, i.e. in the direction of the z axis, it is advantageous to introduce a substitution as referred in [6][7]

$$ds = dz \sqrt{1 + \left(\frac{dx}{dz}\right)^2 + \left(\frac{dy}{dz}\right)^2}.$$
(6)

This leads to two partial differential equations, which can be simplified by assuming a small deviation of the beam from the z axis. Thus

$$\frac{d}{dz} \left(n \frac{dx}{dz} \right) \approx \frac{\partial n}{\partial x}, \quad \frac{d}{dz} \left(n \frac{dy}{dz} \right) \approx \frac{\partial n}{\partial y}.$$
(7)

The second known method is mainly used in plasma physics and is based on the description of the quantum of electromagnetic radiation described by Hamilton's equations[8]

$$\frac{\mathrm{d}\vec{x}}{\mathrm{d}t} = \frac{\partial H}{\partial \vec{p}}, \quad \frac{\mathrm{d}\vec{p}}{\mathrm{d}t} = -\frac{\partial H}{\partial \vec{x}}, \tag{8}$$

where the Hamiltonian function $H = \hbar\omega$ and the momentum $\vec{p} = \hbar\vec{k}$. Since a constant angular frequency ω of the wave is considered, the wave vector depends on the refractive index by the relation $\vec{k} = \vec{k_0}n(x, \vec{y}, z)$, where k_0 is the wave vector in the vacuum. Furthermore, it is possible to introduce a dispersion relation in the form

$$\Theta(\vec{x}, \omega, \vec{k}) = k - k_0 n(x, y, z) = 0, \tag{9}$$

which is directly related to the spatial distribution of the refractive index and $k = \sqrt{(k_x^2 + k_y^2 + k_z^2)}$. Then by replacing the time t with the parameter τ, it is possible to arrive at the equations

$$\frac{\mathrm{d}\vec{x}}{\mathrm{d}\tau} = \frac{\partial \Theta}{\partial \vec{k}}, \quad \frac{\mathrm{d}\vec{k}}{\mathrm{d}\tau} = -\frac{\partial \Theta}{\partial \vec{x}}, \tag{10}$$

where the parameter τ is the geometrical path of the ray, as described in [8], whose differential is described in the equation (6).

Generalized diffraction integral

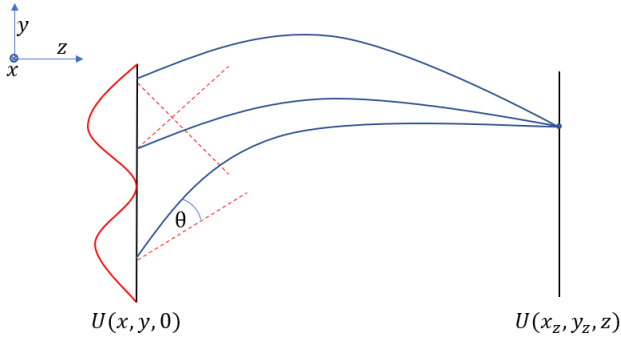$U(x, y, 0)$ $U(x_z, y_z, z)$

Figure 4: Illustration of the generalized diffraction integral principle.

In order to be able to calculate the distribution of the complex amplitude of the optical beam after passing through the non-homogeneous medium to the desired transverse plane, a new method has been developed. The principle of this method generalizes the diffraction integral. Thus, the size of the radius vector r in the equation (3) is replaced by the general Optical Path Length (OPL) of the ray. The effect on the angle θ in the inclination factor is also non-negligible. This is clearly illustrated in the Figure 4. Thus, the angle θ is now not calculated as the angle between the normal vector to the phase and the line connecting the points $[x, y, 0]$ and $[x_z, y_z, z]$, but as the angle between the normal vector to the phase and the derivative

of the ray at the distance $z = 0$. Thus, the generalized diffraction integral can be written by equation

$$\begin{aligned}U(x_z, y_z, z) \\= \frac{i}{\lambda} \iint_{-\infty}^{\infty} U(x, y, 0)\frac{\exp(ikOPL)}{OPL}\cos(\theta)\mathrm{d}x\mathrm{d}y,\end{aligned} \tag{11}$$

with the $OPL = \int n(x, y, z)\mathrm{d}s$, where $\mathrm{d}s$ is the element of the ray from equation(6). The problem with this equation is the necessary knowledge of the trajectory s. This trajectory is a solution to the systems of partial differential equations of (7) or (10). Apart from special cases, these equations do not have an analytical solution and must be solved numerically. In the general case, the beam trajectory of each contribution of the optical field must be solved separately, which will significantly increase the calculation time.

Detection of the Optical beam centre position

In this work 2 types of optical beams, namely GB and SLB are considered. The precise estimation of the center position of the two types of beams was done by the same method. This method uses a known mathematical function whose parameters are optimized to find the best fit to the observed optical beam. A Gaussian function is naturally used for the GB. The Bessel function is used for SLB, which in practice has proven to be very suitable and accurate.

Optical intensity distribution of a GB in the transversal plane is described by the equation

$$\begin{aligned}I_{GB}(x, y) \\= I_{GB0} \exp\left(-4\ln(2)\frac{(x - x_0)^2 + (y - y_0)^2}{FWHM^2}\right),\end{aligned} \tag{12}$$

where I_{GB0} is the optical intensity in the center of the GB, $FWHM$ is the full width of the GB at half maximum value of the optical intensity and points x_0 and y_0 are the coordinates of the center position of the GB. All four variables, i.e. $I_{GB}, FWHM, x_0$ and y_0 are the parameters of the optimization process for finding the best fit with the observed GB.

The function for finding SLB centre position is

$$I_{BB}(x, y) = I_{BB0}\left(\mathrm{J}_0\left(k_T\sqrt{(x - x_0)^2 + (y - y_0)^2}\right)\right)^2, \tag{13}$$

where J_0 is a Bessel function of the first kind and zero order. The parameters to be determined with the optimization process are the optical intensity I_{BB0} of the analytical BB in its center, the transversal wave vector k_T and the coordinates of the center $[x_0; y_0]$.

Conversion of environmental conditions to refraction index

The refraction index, as a basic optical parameter of the environment, generally depends on several variables.
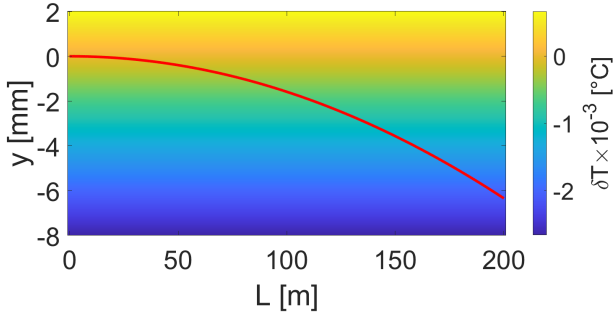
Figure 5: Longitudinal profile of the temperature distribution with the ray trajectory computed by Eikonal equation. The color scale represents the differences of the temperature from the basic value $T_B = 16°C$, so $\delta T = T - T_B$.

The most important variables are wavelength, temperature, pressure, humidity and CO_2 concentration. The wavelength of the beam is constant during propagation. In the range of environmental conditions corresponding to the present cases, the influence of the temperature variations on the change of the refractive index value is one order of magnitude higher than the one due to the pressure gradient. So, in this study, the model is based on the invariance of all parameters except temperature. In this work, the model of real environment is based on temperature measurement data and constant values are defined for the other parameters, so pressure $p = 101325$ Pa, fractional humidity $h = 0$ and CO_2 concentration $C_{CO_2} = 450$ ppm. For the calculation of the refractive index from the environmental parameters a model developed by Philip E. Ciddor [9] have been used.

NUMERICAL SIMULATIONS

Three simulations have been performed for different types of environmental non-homogeneity. On one hand, an environment with a linear temperature dependence on the vertical position and a zero temperature gradient in the other two axes has been considered. The remaining two models used a temperature distribution based on data from measurements in the TT1 and LHC tunnels at CERN. There, a non-zero temperature change in the vertical and longitudinal axis, and a zero temperature gradient in the horizontal axis are considered.

1st model, Linear distribution of the temperature

The temperature at any point in this case depends only on its vertical position along y axis and is given by the relation

$$T(y) = l_1 y + l_2, \tag{14}$$

where the coefficients $l_1 = 1/3$ and $l_2 = 16$. So, an altitude variation of 3 m results in a temperature change of 1 °C. The longitudinal temperature distribution is shown in the Figure 5. A longitudinal profile of the SLB is then shown in the Figure 6. On this picture it is visible that the
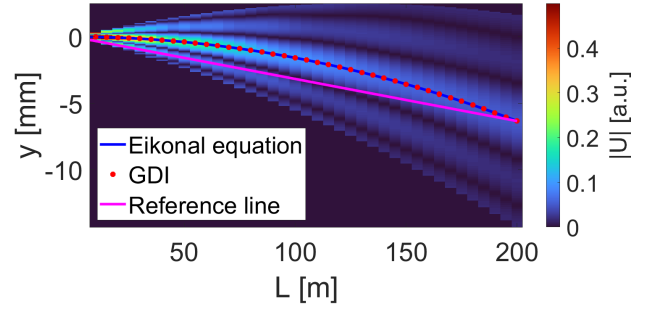

Figure 6: Longitudinal profile of the SLB field amplitude for temperature linearly changing in the vertical axis.
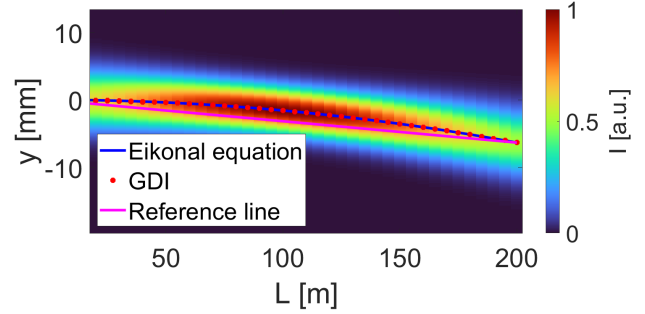

Figure 7: Longitudinal profile of the optimal GB optical intensity for temperature linearly changing in the vertical axis.

trajectory computed by Eikonal equation is nearly identical with the trajectory computed by GDI. The difference is visualized in the Figure 16. The difference Δy is linearly increasing and reaches the values of units of micrometers. This indicates a great agreement between the Eikonal equation and the generalized diffraction integral for the linear dependence of the temperature distribution. An offset of the SLB trajectory from the reference line is visualised in the Figure 17. The reference line is the line joining the start and end points of the trajectory calculated using the Eikonal equation. The maximum value of the offset is close to the centre of the alignment window and is nearly equal to 1.6 mm.
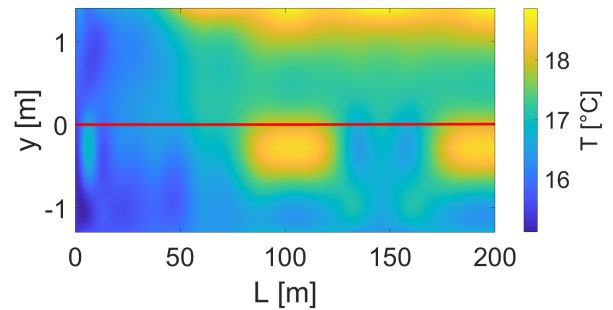

Figure 8: Longitudinal profile of the temperature distribution with the ray trajectory computed by Eikonal equation.
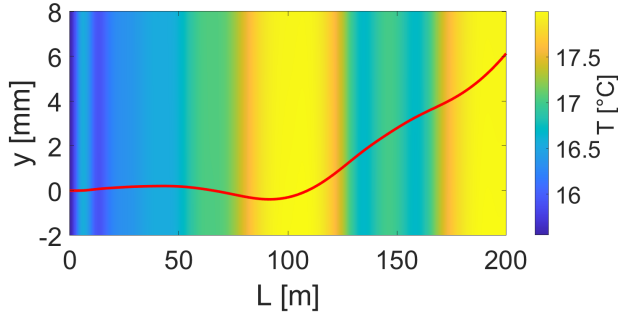
Figure 9: Longitudinal profile of the temperature distribution with the ray trajectory in the near vicinity of the ray.
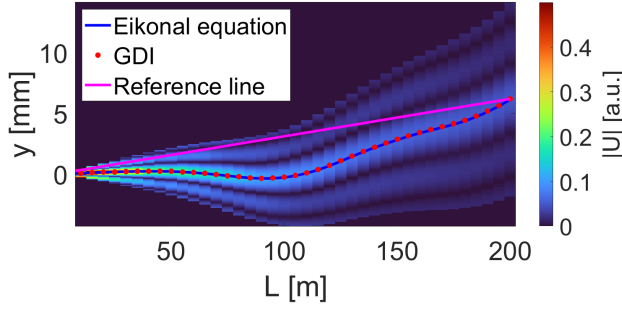

Figure 12: Longitudinal profile of the temperature distribution with the ray trajectory computed by Eikonal equation.

Figure 10: Longitudinal profile of the SLB field amplitude for temperature distribution based on measurement in TT1 tunel.

The propagation of the optimal GB was also simulated under the same conditions. The longitudinal profile is shown in the Figure 7. The differences Δy at each longitudinal distance between results from Eikonal equation and from GDI are visualised in the Figure 16. The offset of the GB trajectory from the reference line is shown in the Figure 17.

2nd model, data from real measurement

The data of the temperature distribution used in this model are based on measurements done in TT1 tunnel. The

temperature distribution is shown in the Figure 8 and includes the ray trajectory computed by Eikonal equation. Obviously the vertical scale of the picture on the Figure 8 is too large, so the Figure 9 shows the temperature distribution in the near vicinity of the ray. The SLB development profile, computed by generalized diffraction integral, is shown in the Figure 10. The SLB trajectory is, as expected, more complicated. In this case, the comparison of trajectories calculated using the Eikonal equation and the generalized diffraction integral is interesting. The differences Δy are visible in the Figure 16 and they exceed the value 50 μm. The offset of the SLB trajectory from the reference line is shown in the Figure 17.

The propagation of the optimal GB was also simulated under the same conditions. The longitudinal profile is shown in the Figure 11. The differences in each longitudinal distances between results from Eikonal equation and GDI are visualised in the Figure 16. The offset of the GB trajectory from the reference line is visualised in the Figure 17.

3rd model, data from real measurement

The data of the temperature distribution used in this model are based on the measurement done in LHC at CERN. The temperature distribution in that case is shown in the Figure 12. The large scale of the temperature map makes it impossible to see the details of the beam trajectory. The Figure 13 shows the same temperature map, but
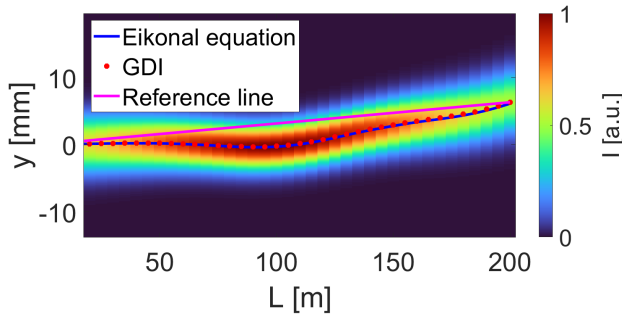

Figure 11: Longitudinal profile of the optimal GB optical intensity for temperature distribution based on measurement in TT1 tunel.
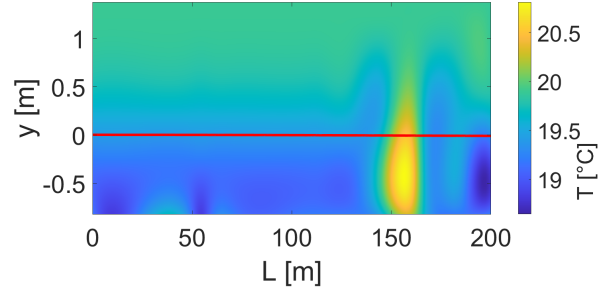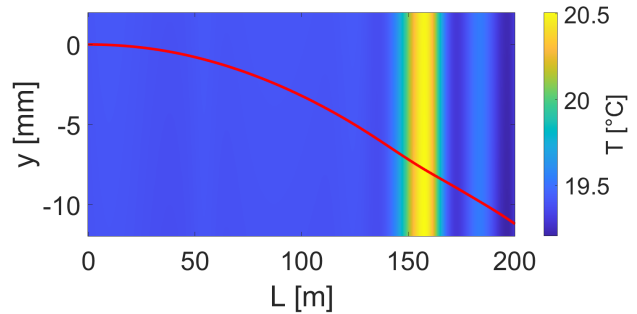

Figure 13: Longitudinal profile of the temperature distribution with the ray trajectory in the near vicinity of the ray.
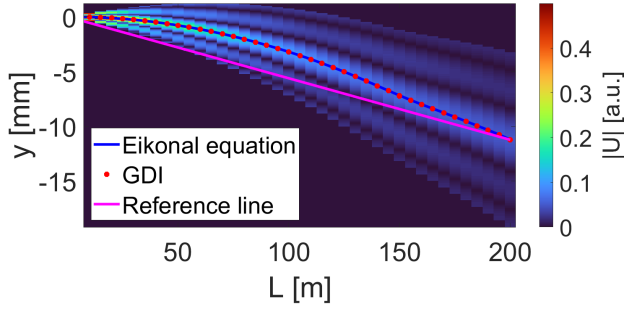
Figure 14: Longitudinal profile of the SLB field amplitude for temperature distribution based on measurement in LHC tunel.

in the near vicinity of the SLB. The trajectory has again non-trivial shape and the longitudinal profile is shown in the Figure 14.

The propagation of the optimal GB was also simulated under the same conditions. The longitudinal profile is shown in the Figure 15. The differences Δy at each longitudinal distance between results from Eikonal equation and GDI are visualised in the Figure 16. The offset of the GB trajectory from the reference line is shown in the Figure 17.
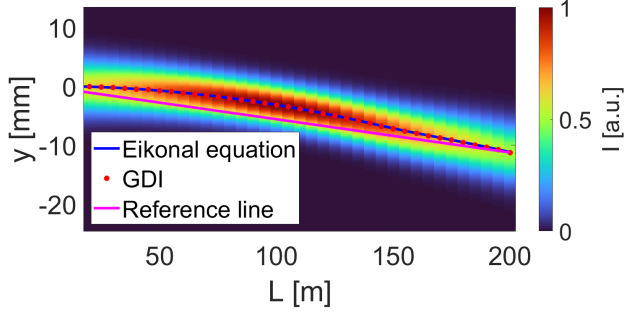

Figure 15: Longitudinal profile of the optimal GB optical intensity for temperature distribution based on measurement in LHC tunel.

DISCUSSION OF RESULTS

As part of the evaluation of the results, attention is focused on two aspects. One is a comparison of both methods of tracing the trajectory of optical beams. The GDI method provides very similar results to the Eikonal equation on scales not smaller than units of millimeters, which is consistent with the theoretical assumption. Non-negligible differences are observable when reducing the observation scale to tens of micrometers. This is perfectly visible in the Figure 16, where the value on the y-axis is the difference between the value of the trajectory position computed by Eikonal equation y_{Eik} and the value of the SLB center position detected by fitting method from the optical field simulated by GDI method y_{GDI}, so $\Delta y = y_{Eik} - y_{GDI}$.
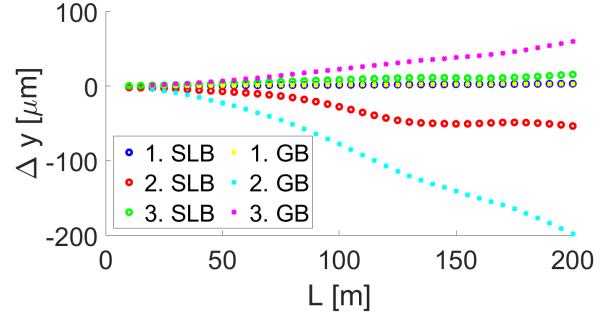

Figure 16: Differences Δy of the vertical positions along the alignment window between trajectories computed by Eikonal equation and by GDI in the 3 models (1, 2 and 3 in the legend). So $\Delta y = y_{Eik} - y_{GDI}$.

An interesting fact is that for the first model with a linear temperature dependence, the largest observed difference Δy is very small (approximately 3 μm) and is the same for the SLB and GB models. In other cases, when the temperature distribution has a general character, the differences reach non-negligible values in the order of several tens of micrometers.
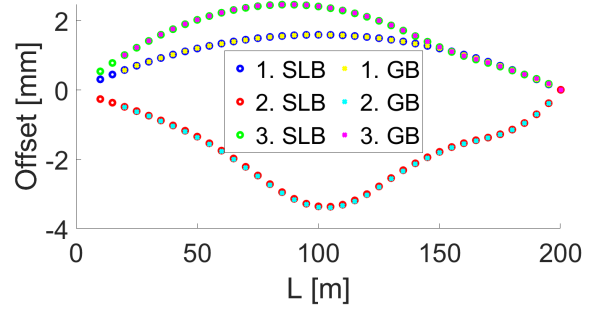

Figure 17: The offsets of the optical beams trajectories from the reference line computed by GDI in the 3 models (1, 2 and 3 in the legend). The sign is given by the relative position of the given point to the reference line on the vertical axis.

Significantly larger differences Δy are observed for the same temperature model with GB than with SLB. In the second temperature model, the difference Δy for the GB even exceeds the value of 200 μm in amplitude at distance $L = 200$ m, while difference Δy for SLB in the same conditions has an amplitude approximately equal to 53 μm. The reason for this fact is unclear.

The second aspect discussed is the offset of the actual trajectory from the expected reference line. Naturally, the offset values for both types of beam almost overlap in each model, see Figure 17. The offset was calculated so that its sign is positive if the actual value of the position of the optical beam is deviated in the positive direction of the y-axis from the assumed reference line. On the given dimensional scale, 200 m long alignment window, the deviations

are similar in amplitude and reach values in the order of lower units of millimeters.

CONCLUSION

A new method for tracing optical fields through non-homogeneous environments based on the wave principle of optics has been developed. The traced entity is a complex amplitude from which the optical intensity is easily calculated. This provides the possibility to calculate the shape of any optical beam, unlike existing conventional methods such as Eikonal equation or Ray tracing. While the trajectory calculated by conventional methods informs about the assumed position of the centre of the optical beam, GDI provides the optical intensity distribution on which the centre position is subsequently detected.

Regardless of the used trajectory calculation method, the maximum offset from the reference line in realistic conditions was about 3 mm. That shows to the importance to consider the medium according to the alignment needs.

In the conditions described above, the observed results show a small, yet noticeable deviation from the trajectory computed by conventional methods and from the detected beam center computed by GDI. These deviations generally increase non-linearly with distance. On a given 200 m long alignment window, they reach values in the order of tens of micrometers for SLB and few hundreds of micrometers for GB, which represents units of percent of the total offset from the reference line.

This new method is able to help finding the optimal design in an alignment project using SLB. It will help deciding whether or not it is necessary to propagate the SLB under vacuum, whether or not it is necessary to propagate the SLB through a tube, what are the free space requirements around the SLB, etc.

ACKNOWLEDGMENT

REFERENCES

[1] D. M. Gale, "Visual alignment of mechanical structures using a bessel beam datum: practical implementation," in *Optical Measurement Systems for Industrial Inspection VII*, vol. 8082, pp. 1013–1024, SPIE, 2011.

[2] R. E. Parks, "Aligning reflecting optics with bessel beams," in *Optical System Alignment, Tolerancing, and Verification XIII*, vol. 11488, pp. 144–154, SPIE, 2020.

[3] R. E. Parks, "Practical considerations for using grating produced bessel beams for alignment purposes," in *Optomechanics and Optical Alignment*, vol. 11816, pp. 11–18, SPIE, 2021.

[4] J.-C. Gayde and M. Sulc, *An Optical System for Producing a Structured Beam*. EP3564734, 2019.

[5] J.-C. Gayde, K. Polak, and M. Sulc, "Introduction to structured laser beam for alignment and status of the R&D," 2022.

[6] M. Born and E. Wolf, *Principles of optics: electromagnetic theory of propagation, interference and diffraction of light*. Elsevier, 2013.

[7] B. E. A. Saleh and M. C. Teich, *Fundamentals of Photonics*. Wiley Series in Pure and Applied Optics, Wiley-Blackwell, 3 ed., mar 2019.

[8] P. Kulhánek, *Úvod do teorie plazmatu*. AGA, 2020.

[9] P. E. Ciddor, "Refractive index of air: new equations for the visible and near infrared," *Appl. Opt.*, vol. 35, pp. 1566–1573, Mar. 1996.